

Analysis of Electron and Muon Size Spectra of EAS

R. Glasstetter^{1*}, T. Antoni², W.D. Apel², F. Badea³, K. Bekk², K. Bernlöhr², E. Bollmann²,
 H. Bozdog³, I.M. Brancus³, A. Chilingarian⁴, K. Daumiller¹, P. Doll², J. Engler², F. Feßler², H.J. Gils²,
 R. Haeusler², W. Hafemann², A. Haungs², D. Heck², J.R. Hörandel^{1†}, T. Holst², K.-H. Kampert^{1,2},
 J. Kempa⁵, H.O. Klages², J. Knapp^{1‡}, H.J. Mathes², H.J. Mayer², J. Milke², D. Mühlenberg²,
 J. Oehlschläger², M. Petcu³, H. Rebel², M. Risse², M. Roth², G. Schatz², F.K. Schmidt¹, H. Schieler²,
 T. Thouw², H. Ulrich², A. Vardanyan⁴, B. Vulpesu³, J.H. Weber¹, J. Wentz², T. Wibig⁵, T. Wiegert²,
 D. Wochele², J. Wochele², J. Zabierowski⁶,

¹*Institut für Experimentelle Kernphysik, University of Karlsruhe, D-76021 Karlsruhe, Germany*

²*Institut für Kernphysik, Forschungszentrum Karlsruhe, D-76021 Karlsruhe, Germany*

³*National Institute of Physics and Nuclear Engineering, RO-7690 Bucharest, Romania*

⁴*Cosmic Ray Division, Yerevan Physics Institute, Yerevan 36, Armenia*

⁵*Department of Experimental Physics, University of Lodz, PL-90950 Lodz, Poland*

⁶*Soltan Institute for Nuclear Studies, PL-90950 Lodz, Poland*

Abstract

The electron and muon numbers of extensive air showers in the energy region around the knee are measured by the detectors of the KASCADE array. To understand the resulting size spectra one has to take into account the fluctuations of the shower development in the atmosphere as well as the uncertainties of the applied reconstruction methods. A consistent interpretation of both spectra allows to derive a primary energy spectrum and a mass composition.

1 Introduction:

The KASCADE–Experiment (Klages et al., 1997) at the *Forschungszentrum Karlsruhe* (110m a.s.l., Germany) was designed to determine the different particle numbers and distributions in an extensive air shower (EAS) in quite a number of ways in the energy region around the so-called *knee* (10^{14} - 10^{17} eV). Therefore, it consists of a $200 \times 200 \text{m}^2$ scintillator array with 252 detector stations for the detection of the extensive electron and muon component and a $16 \times 20 \text{m}^2$ central sampling calorimeter for the measurement of individual hadrons. Additionally, there are multiwire proportional chambers and streamer tubes for muon tracking. The various types of particle detection minimize ambiguities which arise from the large fluctuations in the shower development. They enable us to derive the energy and mass of the primary particle on an event-by-event basis via multiparameter analysis methods.

A different approach, which is used in this analysis, is to look at the spectra of electron and muon numbers as they are measured by the KASCADE–array and derive the primary energy spectrum from these. This is possible since the energy spectra of different primary particles transform differently to the size spectra; the muon number of an EAS is increasing with primary mass, whereas the electron number is decreasing.

However, in any analysis the shower development fluctuations as well as the reconstruction errors have to be known quantitatively to account for systematical errors, especially if dealing with steep power law spectra.

The spectra used for this analysis are based on a data set measured from Oct. 1996–Nov. 1998 with over 12 Mio. reconstructed events in a zenith angle interval from 18° to 25° . The so-called *truncated* muon number $N_{\mu, tr}$ used in the following denotes the integrated number of muons in the region from 40m to 200m around the core, whereas the electron number N_e is reconstructed over all radial distances.

*corresponding author; e-mail: ralph@ik1.fzk.de

†present address: University of Chicago, Enrico Fermi Institute, Chicago, IL 60637

‡now at: University of Leeds, Leeds LS2 9JT, U.K.

2 Mathematics:

The influence of any type of fluctuations on a certain distribution of observables or even just the transformation of one observable to another is described by a *Fredholm integral equation of 1st kind*:

$$\frac{dJ_i}{d \lg N_j} = \int_{-\infty}^{\infty} \frac{dJ_i}{d \lg E} p_i(\lg E \rightarrow \lg N_j) d \lg E \quad \text{with } i = p, \dots, fe \text{ and } j = e, \mu \quad (1)$$

The lefthand side represents the evaluated size spectra for various primaries i , and the so-called *kernel* function p_i is the probability for a primary of the given energy E that an air shower is reconstructed with a certain shower size N_j .

Actually it is helpful to factorize the kernel function to reflect the stages of shower development, detector sampling and reconstruction:

$$p(\lg E \rightarrow \lg N_j) = \int_{-\infty}^{\infty} p_{dev}(\lg E \rightarrow \lg N'_j) p_{eff}(\lg N'_j) p_{rec}(\lg N'_j \rightarrow \lg N_j) d \lg N'_j \quad (2)$$

with the probability p_{dev} , that a shower arrives at the observation level with given size N' , the trigger efficiency p_{eff} , which depends mainly on the number of detected particles and the probability p_{rec} , taking into account the statistical and systematical reconstruction errors.

To solve equation (1) for the primary spectrum dJ_i/dE an appropriate parameterization of the primary spectrum is done and the spectral parameters are estimated by fitting the theoretical distribution (1) to the measured size spectra. This method allows us to use the additional information that the primary spectrum obeys a power law. In the following analysis the primary energy spectrum is parameterized as a function of five parameters. The spectral indices $\gamma_{1,2}$ below and above the knee, the position of the knee E_k , the flux at the knee dJ/dE_{knee} and the width of the knee ΔE , which describes the region around the knee, where the spectral index is changing from γ_1 to γ_2 .

3 Fluctuations:

To determine the above kernel functions one needs detailed information about the dependence of fluctuations on primary energy resp. showers size for the various primary particles. The shower simulation code CORSIKA (Heck et al., 1998) was used with the interaction model OGSJET to obtain the necessary data. To minimize the amount of simulations the MC data set was limited to proton and iron primaries with a zenith angle of 22° . For the study of the shower development fluctuations and the average dependence of shower size upon primary energy the *thinning* option of CORSIKA was used which allowed the generation of an appropriate large number of individual showers from 3×10^{13} eV up to 10^{17} eV. A different data set of full simulated showers from 10^{14} eV to 10^{16} eV was used to get the detector responses from a detailed detector monte carlo. These responses were analyzed in the same way as the experi-

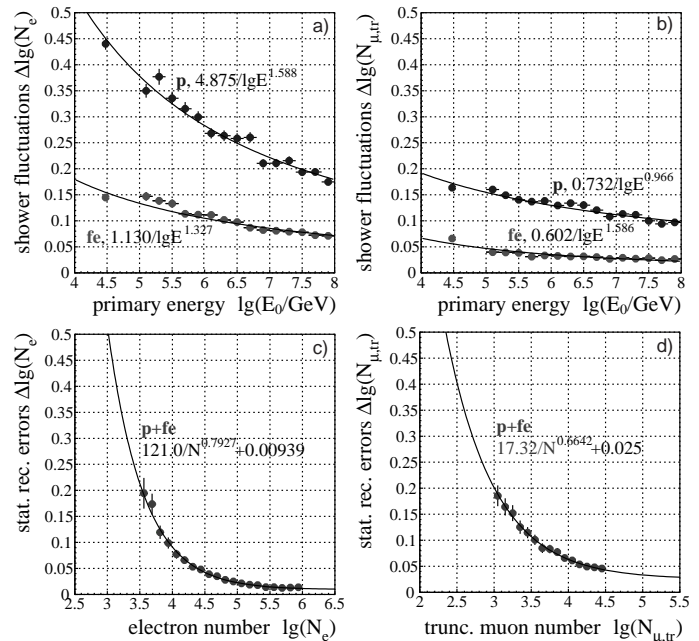


Figure 1: Shower development fluctuations and statistical reconstruction errors of shower sizes.

mental data by the KASCADE reconstruction code to get the statistical and systematical errors of the reconstruction as well as the efficiencies.

Figure 1 shows the parameterized standard deviations resulting from this analysis. Both kind of fluctuations are well described by a normal distribution on a logarithmic scale. Since the statistical errors do not depend significantly on the type of the primary, only one function is used for the parameterization. It can be seen that for protons the shower fluctuations always are dominating, whereas for iron induced showers those are reduced by a factor of about 3. Therefore the statistical errors become important, especially for the muon component of small showers.

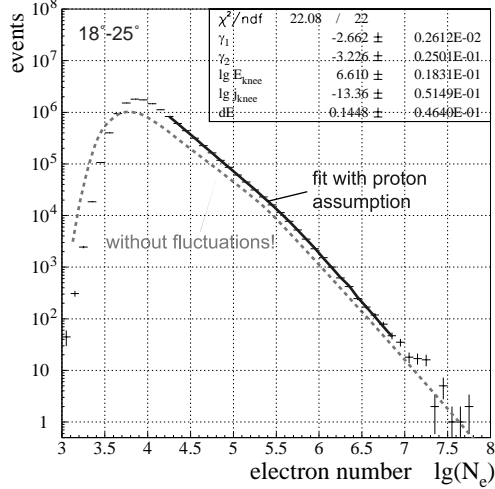


Figure 2: Fit of shower size spectrum including proton fluctuations.

Figure 2: Fit of shower size spectrum including proton fluctuations. The knee positions are also at smaller values, hence, the primary fluxes at the knee have become larger. Nevertheless, the fluxes and spectral indices above the knee, derived separately from the electron and muon spectra with these assumed pure compositions, are still inconsistent even with fluctuations taken into account.

To illustrate the effect of the fluctuations in Fig. 2, the fit of the electron size spectrum using the proton kernel function and the resulting energy spectrum parameters are plotted. The data are as well described as in former analyses (Glasstetter et al., 1998) where the size spectra directly were parameterized by two power law functions. Now the fluctuations have been taken into account and the values of the parameters have changed significantly. The dashed line shows the hypothetical spectrum that would have been measured with the quoted primary parameters and fluctuations *switched off*.

In Table 1 the results of direct fits are listed together with the actual ones, which are obtained by separate fits to the electron and truncated muon spectra assuming a pure proton or iron composition. Fit errors are not given because the systematical errors by assuming the wrong composition are at least a factor of 10 larger than the statistical ones. As one can see the primary spectral indices have become smaller by 0.1-0.2. The knee positions are also at smaller values, hence, the primary fluxes at the knee have become larger.

		PROTON				IRON			
		γ_1	γ_2	E_{knee}	dJ_{knee}/dE	γ_1	γ_2	E_{knee}	dJ_{knee}/dE
no	N_e	-2.83	-3.42	5.6	$2.5 \cdot 10^{-14}$	-2.85	-3.44	11.	$1.3 \cdot 10^{-14}$
fluct.	$N_{\mu, tr}$	-2.88	-3.04	4.7	$5.2 \cdot 10^{-14}$	-2.88	-3.04	3.7	$6.6 \cdot 10^{-14}$
incl.	N_e	-2.66	-3.22	4.0	$4.7 \cdot 10^{-14}$	-2.84	-3.31	9.0	$2.1 \cdot 10^{-14}$
fluct.	$N_{\mu, tr}$	-2.58	-2.99	3.0	$16 \cdot 10^{-14}$	-2.69	-3.02	3.5	$7.1 \cdot 10^{-14}$

Table 1: Comparison of primary energy spectra fit parameters derived independently from electron and muon spectra assuming pure compositions (E_{knee} in PeV and dJ_{knee}/dE in $\text{m}^{-2}\text{s}^{-1}\text{sr}^{-1}\text{GeV}^{-1}$).

4 Spectra and Composition:

The above analyses have shown that it is obviously impossible to describe the observed size spectra by any pure composition in a consistent way. On the other hand, using the presented fitting procedure there is no reason anymore to fit the size spectra separately. Therefore, a combined χ^2 -minimization has been chosen to fit both size spectra simultaneously:

$$\chi^2 = \sum_{j=e}^{\mu} \sum_{k=n_{min,j}}^{n_{max,j}} \left(\frac{dJ/d \lg N_j \cdot \Delta \lg N_j - J_{j,k}}{\sqrt{J_{j,k}}} \right)^2 \quad (3)$$

The $J_{j,k}$ represent the number of events in the bin k with width $\Delta \lg N_j$ and the theoretical functions $dJ/d \lg N_j$ are now the sum over the Fredholm integrals (1) for the two extreme primary particles (p and Fe), which should be taken as representatives for a light and heavy group of primary particles.

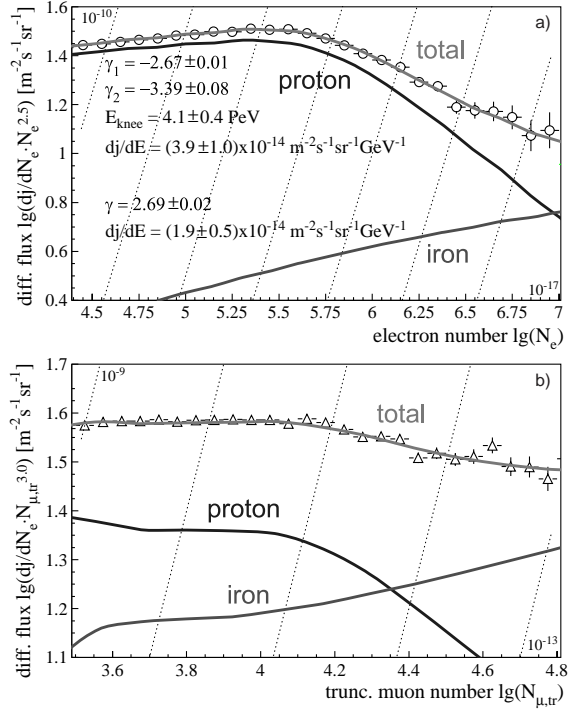


Figure 3: Electron and trunc. muon size spectra fitted simultaneously with a two-component composition ($\vartheta = 18^\circ - 25^\circ$).

ranges in Fig. 3, the lines outside are extrapolated. Below the knee at approx. 4PeV there is a nearly constant composition with 30% heavy contributions. This changes above the knee at 10^{16} eV to 50% and at 10^{17} eV even to 80%. The total flux in that region coincides well with values of other experiments and the generally accepted values for the spectral indices.

If the heavy component would proceed with that behavior, then the all-particle spectrum above 10^{17} eV should become flatter as the extrapolated straight line indicates. This would be in disagreement with most experiments performed in that region, whereas a rigidity like cut-off of the iron component due to the escape of the particles from the galaxy at around $26 \times E_{k,proton}$ with an index of 3.1 (dashed line) fits the data.

To reduce the number of free parameters, the width of the knee was fixed to $\Delta E = \pm 0.15$, which resulted from the single spectra fits. There are 8 free parameters: the spectral indices, the knee position and the flux at the knee for each primary. An first attempt has shown that the spectral index of the iron component above the knee with respect to the fit error is nearly identical to the index below the knee with an very large error on the *knee position*. Therefore, the final fit was performed with a six parameter function, describing the iron component as a single power law without any bend in slope within the fitted region.

The resulting primary parameters with statistical errors are plotted in Figure 3 together with the underlying size spectra. The dotted lines represent lines of constant flux, with the maximum and minimum values plotted in the corners. Despite our simplifications both spectra are described very well over the whole range ($\chi^2/ndf=1.14$). The electron size spectrum (a) is dominated by the proton component, which is responsible for the steep slope above the knee, whereas the trunc. muon number spectrum (b) reflects more the behavior of the total energy spectrum.

Figure 4 shows the parameterized primary energy spectra. The grey shaded regions correspond to the fitted

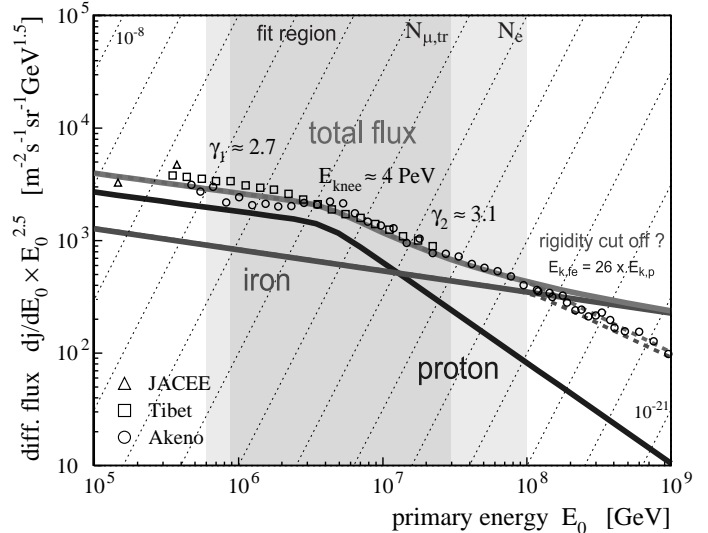


Figure 4: Energy spectra resulting from the simultaneous fit of electron and trunc. muon spectra.

References

- Glasstetter, R., Hörandel, J.R. et al., 1998, Proc. 16th ECRS, Alcalá, 559
 Heck, D. et al., 1998, FZKA 6019, Forschungszentrum Karlsruhe
 Klages, H.O. et al., 1997, Nucl. Phys. B (Proc. Suppl.), 52B 92